PHYSICAL REVIEW E **73**, 041409 (2006)

Colloid interaction and pair correlation function of one-dimensional colloid-polymer systems

C.-Y. Chou,[1] B. Payandeh,[1] and M. Robert[1,2]
[1]*Department of Chemical and Biomolecular Engineering, Rice University, Houston, Texas 77005, USA*
[2]*Rice Quantum Institute, and Richard E. Smalley Institute for Nanoscale Science and Technology, Rice University, Houston, Texas 77005, USA*

(Received 5 May 2005; revised manuscript received 1 March 2006; published 28 April 2006)

The interaction and pair correlation function of weakly charged colloidal particles in quasi-one-dimensional colloid-polymer systems are determined by enhanced video microscopy and digital image analysis. The pair correlation function is found to depend not only on the polymer concentration, but also on the degree of confinement; in particular, it depends on whether the channel width is such that mutual passage of the colloid particles is possible or not. These findings are compared with exact results on short-range order in linear continuous systems.

DOI: 10.1103/PhysRevE.73.041409 PACS number(s): 82.70.Dd, 05.40.Jc, 61.25.Hq

I. INTRODUCTION

While studies of colloid and colloid-polymer systems have traditionally been concerned with bulk three-dimensional systems [1–6] for either charged [7–10] or neutral [11,12] colloid particles, recent investigations have focused on colloid particles in confined geometries [13–25]. For mixtures of colloidal particles and for colloid-polymer systems, the size difference of the components is well known to lead to depletion interactions, which are generally attractive. Theoretical studies of depletion effects in one-dimensional geometries have dealt with the thermodynamic properties of hard rods mixtures [26] and pair correlation functions [27]. It appears, however, that experimental knowledge of colloid-polymer mixtures in one-dimensional geometries is lacking.

Colloid particles in confined geometries, unlike those in a bulk three-dimensional environment, can be tracked with the aid of video microscopy [17], so that their static and dynamic properties can be readily obtained. Of particular interest is the pair correlation function which, according to statistical mechanics, determines the thermodynamic properties of the colloid suspension as well as the colloidal interaction. Indeed, as is well known, the latter can be determined from the pair correlation function in the dilute regime:

$$h(x) = \exp[-U(x)/k_BT] - 1, \qquad (1)$$

with $h(x)$ the pair correlation function, x the separation between the centers of mass of two colloidal particles, U the interaction potential, k_B Boltzmann's constant, and T the absolute temperature.

In the present study, the colloid pair correlation functions and interactions for colloid-polymer systems are investigated experimentally in one-dimensional channels by enhanced video microscopy and computer image analysis. The experimental method is described in Sec. II, the results are presented in Sec. III, and their discussion is given in Sec. IV, followed by a conclusion in Sec. V.

II. EXPERIMENTAL METHOD

The present experimental study of one-dimensional colloid-polymer systems is performed by confining these systems in channels, which can be made sufficiently narrow that mutual passage of colloidal particles is impossible. Colloid particle positions are recorded by video microscopy onto video tapes after settling in the confined channels for 6 h. The procedures start with the fabrication of cells of one-dimensional channels, dispensing of colloid-polymer solutions in the channels, and finally movie recording and image processing.

A. Preparation of colloid-polymer solutions

The colloid system studied in the present work is an aqueous solution of silica particles (diameter $\sigma = 1.58 \pm 0.04$ μm, density $= 2.18$ g/cm^3, Duke Scientific). The negatively charged silica particles are dispersed in de-ionized water (specific resistance 18 MΩ cm, Millipore) to yield solutions of 0.0025, 0.006, 0.012, and 0.02 wt %. Extra care is exercised with the addition of polymer in the colloid suspension. Poly(ethyleneoxide) (PEO, Aldrich Inc.) with a molecular weight of 8 000 000 is chosen as the polymer. The nonionic surfactant polyoxyethylene glycol $C_{12}E_8$ is introduced in the colloid solution before adding polymer, to prevent polymer adsorption on the silica particles. The surfactant molecules and colloid particles are well mixed on a rotating drum for 4 h. The concentration of the surfactant is fixed for all measurements and is chosen to be equal to 95% of the critical micelle concentration. Finally, the PEO solution is added and rolled on the rotating drum overnight.

B. Cell of one-dimensional channels

The cells are described in detail in our recent study of Ref. [28] and are illustrated in Fig. 1 of that latter paper. The quasi-one-dimensional channels are provided by the Microtechnology Laboratory of the University of Minnesota. The features of the channels are printed on silicon wafers with the photolithography technique followed by dry etching. Prior to making patterns out of silicon wafers, each wafer is first

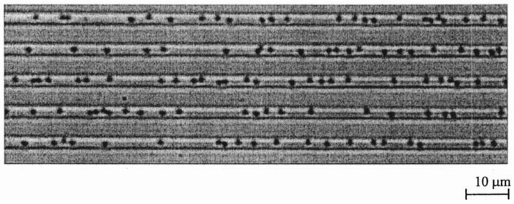

FIG. 1. Snapshot of colloid particles dispersed in quasi-one-dimensional channels.

cleaned by heating at 90 °C in a piranha solution, a mixture of 30% H_2O_2, and concentrated H_2SO_4 (30:70 v/v) and subsequently treated with the silanizing reagent octadecyltrichlorosilane (OTS) solution [29]. The procedure to fabricate one-dimensional grooves from the master silicon wafer is standard (see, for example, [24]). The sylgard 184 elastomer base and its curing agent (Dow Corning) are well mixed to achieve a transparent elastomeric polymer, poly-(dimethysiloxane) (PDMS). In contrast to the design of Ref. [24], the perimeter walls are raised so that a deep reservoir (500 μm in depth) is created above the top surfaces of the channels. The sample cells are created by dispensing colloid solutions into the channels and covering them with slips, which are treated so as to be hydrophobic [30]. A photograph of the system of narrow channels is shown in Fig. 1. All measurements are performed at temperature $T \simeq 25$ °C.

C. Video microscopy and image analysis

The images are recorded into VHS tapes by video microscopy [17]. The magnification of the objective lens is 40×, which gives a resolution of 0.25 μm/pixel. The image analyses include digitizing images with Scion Image, extracting particles information with IDL, tracking particles trajectories, and calculating the pair correlation and nearest-neighbor distribution functions.

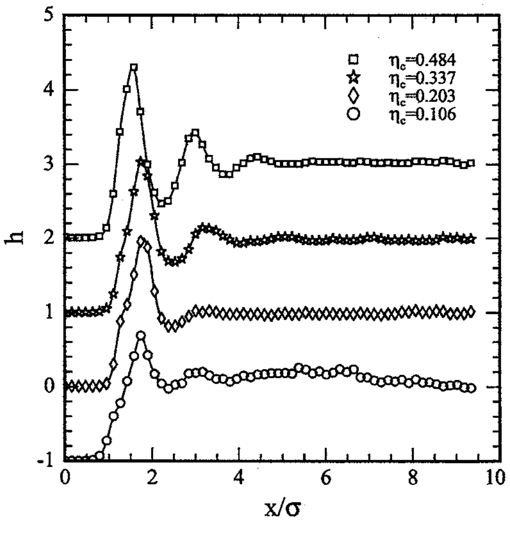

FIG. 2. Pair correlation functions for various colloid concentrations in pure water. For clarity the curves are shifted upward by one unit in this figure as well as in Figs. 3, 4, 6, 7, 9, 10, and 12.

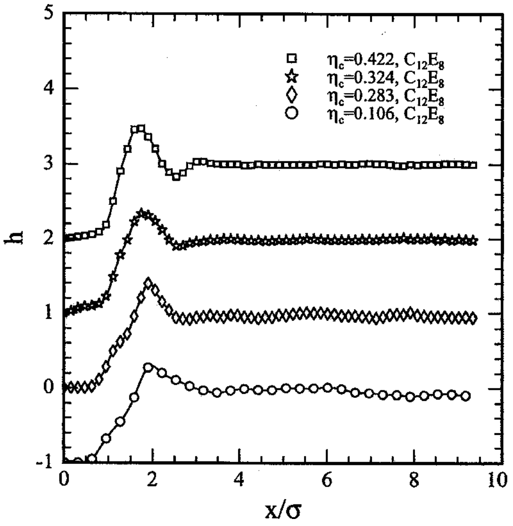

FIG. 3. Pair correlation functions in the presence of the surfactant $C_{12}E_8$.

III. RESULTS

The colloid volume fraction in one dimension is defined as $\eta_c = N\sigma/L$, where N is the number of colloids, σ is the colloid diameter, and L is the length of the channel. The pair distribution function $g(x) = h(x) + 1$ is calculated from the histogram of particle pair separations from each digitized image:

$$g(x) = \rho^{-1} \left\langle \sum_i \sum_j \delta(x_i)\,\delta(x_j - x) \right\rangle = \frac{N(x)}{2\rho\Delta x}, \qquad (2)$$

where $N(x)$ is the average number of particles within distance $x - \Delta x/2$ to $x + \Delta x/2$ from a reference particle and ρ is the average number density. To avoid edge effects, the reference particles for any separation are chosen to be at least a distance x from the edges of the images.

The pair correlation functions of pure silica particles, those of silica particles in presence of surfactant, and those

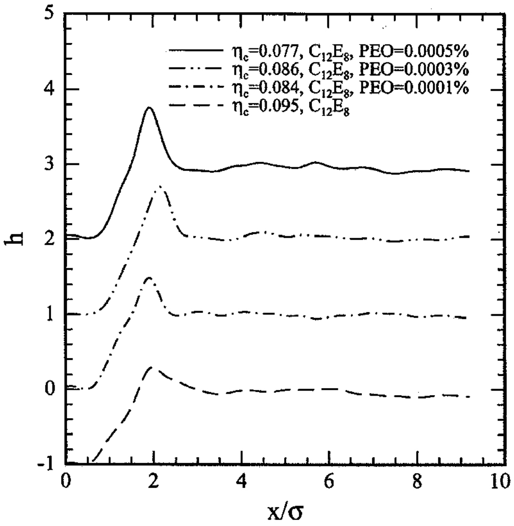

FIG. 4. Pair correlation functions in polymer solutions.

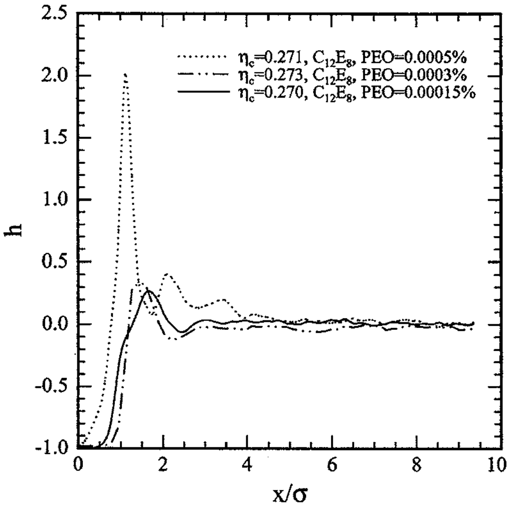

FIG. 5. Pair correlation functions for nearly identical colloid concentrations in polymer solutions of different concentrations in wide channels.

of silica particles-surfactant-polymer solutions are determined. The channel width is chosen to be ~2.75 μm, which is small enough to prevent mutual passing of particles. The pair correlation functions of pure silica colloidal solutions are shown in Fig. 2. The pair correlation functions of colloids in the presence of surfactant and polymer are shown in Fig. 3 and Figs. 4–7, respectively.

In order to study the effects of geometric confinement, the channel width is increased to a width of ~3.48 μm to allow particles to pass each other. Figure 8 illustrates a configuration of colloids in such channels. The colloid pair correlation functions for these wider channels are shown in Fig. 5. They exhibit remarkable new structures. On the one hand, a pronounced colloid ordering, which is not seen for the smaller channel width (see Fig. 4), appears for a 0.0005 wt % PEO solution (see Fig. 5). On the other hand, in Fig. 6, the first peak of the pair correlation function is seen to split into two peaks for a 0.00015 wt % PEO solution.

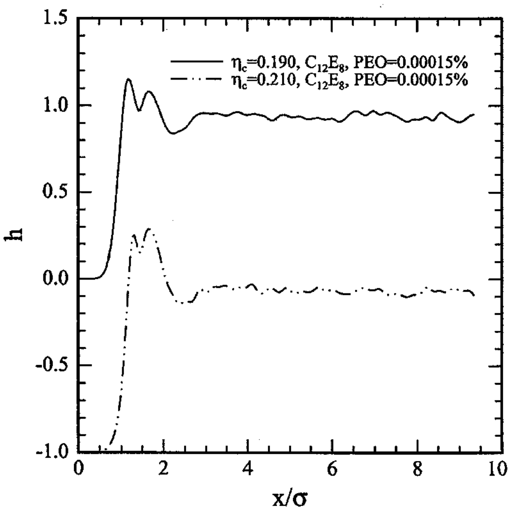

FIG. 6. Pair correlation functions of 0.00015% PEO solution in wide channels.

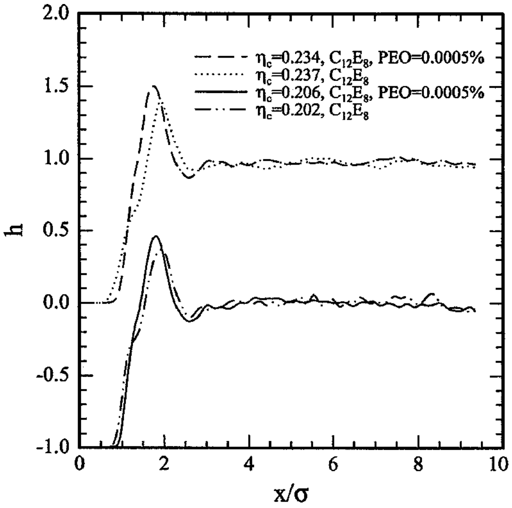

FIG. 7. Pair correlation functions in the absence and presence of polymers in narrow channels.

Another distribution function of interest [24,31–38] is the nearest-neighbor distribution function $H(x)$, defined by

$$H(x)=\sum_i \delta(\min(x_{ij})-x)=\sum_i \delta(\min(x_{i,i-1},x_{i,i+1})-x). \tag{3}$$

The nearest-neighbor distribution function gives the probability, for any given particle, of finding a nearest-neighbor particle at a distance x from that given particle (see Figs. 9 and 10). $H(x)$ is calculated from the histogram of nearest-neighbor separations for each digitized image. Since there is no mutual passing for particles in sufficiently narrow one-dimensional channels, particles retain their initial order and the computational algorithm is simplified.

The interaction potential of silica particles in water without and with polymer, determined from the pair correlation function according to Eq. (1), is shown in Figs. 11 and 12.

IV. DISCUSSION

It is first noted that the present results differ significantly from those of hard rods in one dimension; this is because the competing attractions and repulsions lead to a minimum of the resulting interaction and, correspondingly, to a maximum of the pair correlation function, away from contact. A more detailed discussion of this point is given below.

From Fig. 2, the systems are seen to display more ordered structures as the colloid concentration increases, in accor-

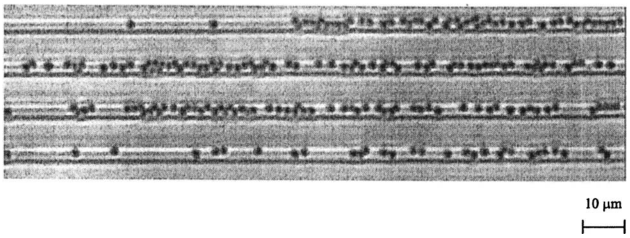

FIG. 8. A configuration of colloids in wide channels.

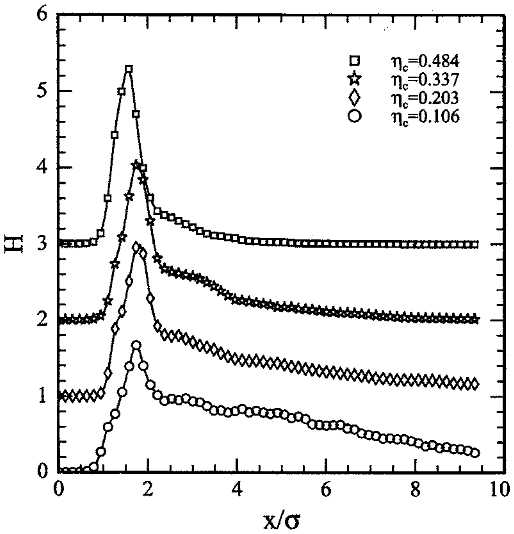

FIG. 9. Nearest-neighbor distribution functions.

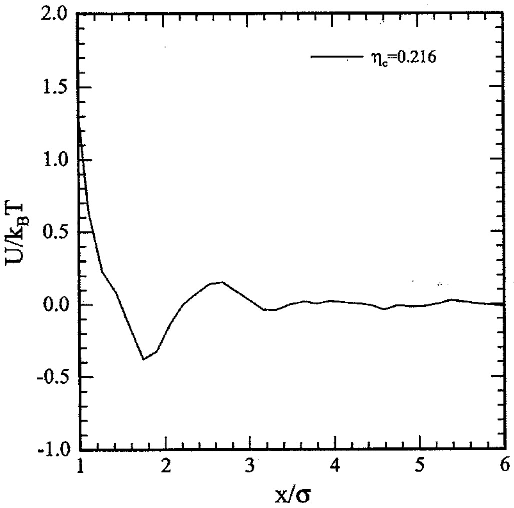

FIG. 11. Colloid interaction potential in narrow channels.

dance with intuition. The displacement of the first peak to a closer pair separation as the packing density increases and the reduction of the ordering structures with the addition of surfactants shown in Figs. 2 and 3, respectively, are consistent with the experimental findings for quasi-two-dimensional geometries [39].

Increasing the polymer concentration amplifies the intensity of the first peak and shifts it to a larger pair separation (see Fig. 4). However, upon further increase of the polymer concentration to 0.0005 wt %, the position of the first peak is displaced to a smaller particle separation, as observed in previous studies [19,23]. At the higher polymer concentration of 0.0005 wt %, the increase of the depletion attraction pushes colloids to closer positions (see Fig. 4). This is further discussed below. It is also noted from Fig. 4 that the correlation function does not vanish for $x/\sigma < 1$. This is because x is not the actual distance between particle centers, but its projection, so that when two particles partially overlap, as they inevitably do in the present quasi-one-dimensional channels, that projected distance is smaller than σ, thus creating a structure in the pair correlation for $x/\sigma < 1$.

The splitting of the first peak of the pair correlation function, shown in Fig. 6, was also found in quasi-two-dimensional binary colloid mixtures [13]. Peak splitting of the pair correlation functions was interpreted there as due to the presence of small colloid particles between two large colloid particles. The individual particle trajectories (not shown) help reveal the distribution of colloids in the channel and indicate that the splitting of the first peak of the pair correlation function corresponds to an inhomogeneous spatial distribution, which results from the uneven dispersion of the polymer inside the channel, similarly to the case studied in Ref. [13].

In general, both the polymer concentration and confinement contribute to the change of the colloidal pair correlation functions. As noted above, the addition of polymer enhances the first peak of the pair correlation functions and shifts it to

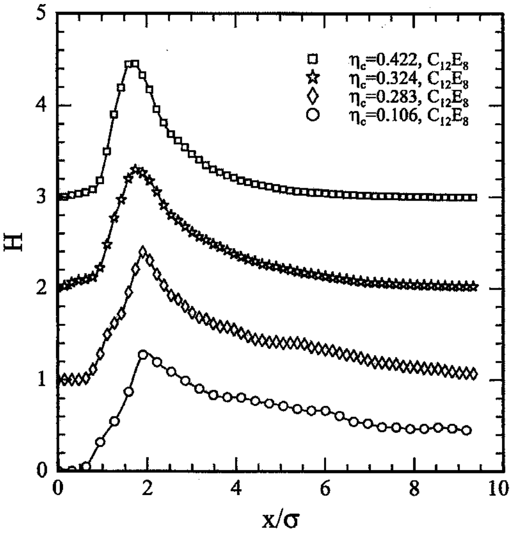

FIG. 10. Nearest-neighbor distribution functions in the presence of the surfactant $C_{12}E_8$.

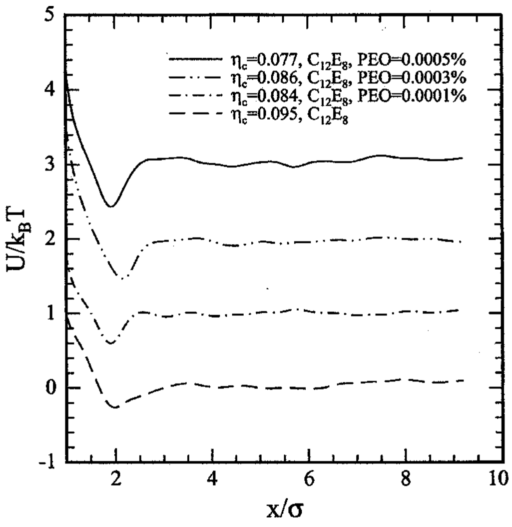

FIG. 12. Colloid interaction potential for various polymer concentrations in narrow channels.

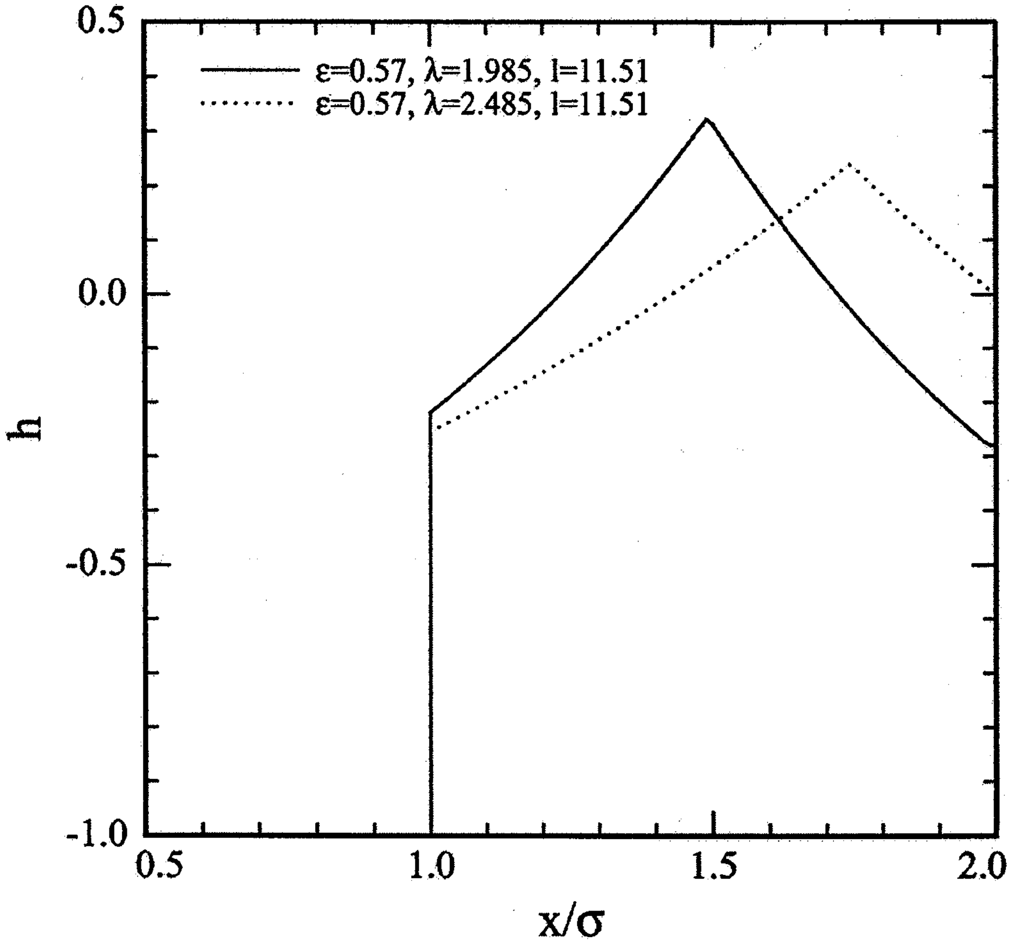

FIG. 13. Pair correlation functions for the V-shaped potential [27] for the interaction parameters obtained from Fig. 12.

a larger or smaller particle separation, depending on the polymer concentration (see Figs. 4 and 7). In their model, Asakura and Oosawa [40] take the polymer to be a sphere of a radius equal to its radius of gyration and the colloid-polymer interaction is assumed to be hard-sphere-like. The depletion force is then found to be proportional to the area of the projection, on the plane perpendicular to the line joining the centers of two neighboring colloids, of the excluded volumes of these particles. The potential minimum occurs at contact, is proportional to the polymer concentration, and decreases with increasing confinement. The shift of the first peak of the pair correlation function seen in the present study accounts for the increase of the depletion interaction as channels become wider. The variation of the potential between the colloids indicates the expected increase of the attraction force due to depletion as the polymer concentration increases [40].

Noteworthy in Fig. 11, which shows the colloid interaction potential in the absence of a polymer, is the weak attraction at short distance (the minimum of the interaction potential, $-0.368k_BT$, occurs at approximately $x/\sigma=1.75$). This attraction can be attributed to several causes: the confinement-induced like-charged attraction [18,41], the van der Waals attraction [42,43] which, together with the screened Coulomb repulsion, forms the basis of the classical DLVO theory [41,44,45], the slight polydispersity of the colloidal particles, and the effective attraction induced by capillary forces [24]. Concerning the latter, because the host liquid does not wet the channel walls, the water-air interface at the bottom of the channels is dimpled by the colloidal particles, generating an effective attraction between them (for a detailed discussion of this effect, see Sec. V of Ref. [24]). The van der Waals attraction can be estimated from the measurements of Crocker *et al.* for single-component colloidal solution (see Fig. 1 of [20]).

These various attractions lead to a minimum in the colloid interaction potential, and as shown in a recent exact analytical study [27] of pair correlations for particles interacting through a potential with an attractive minimum occurring away from contact, the first peak of the correlation function occurs at contact when the attraction depth is small, but moves away from contact to the attractive potential minimum when the attraction depth is large enough; this is precisely what is observed in the Figs. 2–4. In order to make this comparison more quantitative, the parameters of the V-shaped potential of Ref. [27] are obtained from the present experimental data. One finds $\varepsilon=0.57$, $\lambda=1.985$, and $l=11.51$ from Fig. 12 for $\eta_c=0.077$ and PEO=0.0005%. When these values are fit to the exact results of Ref. [27] for a V-shaped potential, one obtains the pair correlation functions at short distances between $x/\sigma=1$ and $x/\sigma=2$ shown in Fig. 13; this figure also shows the case of a longer attraction range. The pair correlation functions resemble closely that of Fig. 4(d) of Ref. [27]. The peak of the pair distribution function occurs away from contact, at the minimum of the potential. It is seen that the relative height of the first peak is smaller due to the weaker attraction depth. It should be noted that the modeling of the potentials of Fig. 12 by a V-shaped potential induces a shift of the potential minimum to a closer distance. This accounts for the difference between Figs. 4 and 13 in the position of the first peak of the correlation functions. These peaks remain located at the minimum of the potential.

The comparison of the colloid interaction potential in one and two dimensions provides more insight into the effects of geometric confinement. In the absence of polymer, no depletion attraction is anticipated and indeed it is found, for the pure colloidal systems studied here, that there is no significant difference between the colloidal interactions in one and two dimensions. For aqueous pure colloidal suspensions in two dimensions, the interaction potential was also determined by other groups, but with slightly differing results [16,20,24]. For example, for fluorescent sulphonate polystyrene spheres of diameter 0.5 μm, the potential depth is found to be $\sim 0.4 k_B T$ [16], while for polymethylmethacrylate (PMMA) spheres of diameter 1.1 μm with large ionic strength, the van der Waals attraction accounts for a potential depth of $\sim 0.2 k_B T$ (see Fig. 1, curve *a* of [20]), and yet another study [24] of silica particles of diameter 1.58 μm reveals an attraction depth of approximately $0.5 k_B T$. By comparison, the attraction depth for the present pure colloidal systems is found to be about $0.35 k_B T$ in two dimensions [39].

In previous experiments on quasi-two-dimensional colloid-polymer systems, it was shown that both the magnitude and range of the depletion potential depend on the polymer concentration [23,46]. The range is governed by the radius of gyration of the polymer in the dilute regime and by the correlation length in the semidilute regime. With the addition of polymer, the first peak of the colloid pair correlation function shifts to larger particle separations and to higher values, as seen in Fig. 4, and correspondingly the minimum of the colloidal interaction potential also shifts to larger particle separations and larger values, as seen in Fig. 12. However, as the polymer concentration is further increased, the first peak of the colloid pair correlation function moves back to short particle distances, as seen in Fig. 4, and correspondingly the colloid interaction minimum is likewise shifted, as seen in Fig. 12; the results are in agreement with previous findings in quasi-two-dimensional systems [19,23]. This behavior is due to the shrinking of the depletion region between neighboring colloidal particles resulting from polymer overlap in the semidilute regime.

V. CONCLUSION

The addition of polymer and presence of geometric confinement are found to significantly alter the structural properties of colloid suspensions. The pair correlation function of the colloid particles indicates that the particles become more correlated in the presence of a polymer. Geometric hindrance also contributes to induce attraction forces between like-charged particles and increases the range of the interaction potentials in the dilute regime. However, the range of the depletion potential is reduced as the polymer concentration enters the semidilute regime.

When more than one layer of colloids is allowed in the channel, clustering of particles is observed due to depletion effects, which is not seen for the monolayers of colloids. The microstructure thus results from the interplay between polymer concentration and geometric confinement.

ACKNOWLEDGMENTS

We thank Dr. Bianxiao Cui for generous discussions on channel fabrication, the National Science Foundation (under Grant Nos. CTS-9700147 and CTS-0327487), and the Welch Foundation (Houston, TX) for financial support.

---

[1] A. Vrij, Pure Appl. Chem. **48**, 471 (1976).

[2] A. P. Gast, C. K. Hall, and W. B. Russel, J. Colloid Interface Sci. **96**, 251 (1983).

[3] B. Vincent, J. Edwards, S. Emmett, and R. Croot, Colloids Surf. **31**, 267 (1988).

[4] H. N. W. Lekkerkerker, W. C. K. Poon, P. N. Pusey, A. Stroobants, and P. B. Warren, Europhys. Lett. **20**, 559 (1992).

[5] S. M. Ilett, A. Orrock, W. C. K. Poon, and P. N. Pusey, Phys. Rev. E **51**, 1344 (1995).

[6] M. Dijkstra, J. M. Brader, and R. Evans, J. Phys.: Condens. Matter **11**, 10079 (1999).

[7] W. Hartl and H. Versmold, J. Chem. Phys. **80**, 1387 (1984).

[8] R. Krause, B. D'Aguranno, J. M. Mendez-Alcaraz, G. Nagele, R. Klein, and R. Weber, J. Phys.: Condens. Matter **3**, 4459 (1991).

[9] G. Nagele, O. Kellerbauer, R. Krause, and R. Klein, Phys. Rev. E **47**, 2562 (1993).

[10] W. Hartl, C. Beck, and R. Hempelmann, J. Chem. Phys. **110**, 7070 (1999).

[11] P. N. Segre, O. P. Behrend, and P. N. Pusey, Phys. Rev. E **52**, 5070 (1995).

[12] V. Degiorgio, R. Piazza, and R. B. Jones, Phys. Rev. E **52**, 2707 (1995).

[13] M. C. M. Tam, S. A. Rice, and A. H. Marcus, Chem. Phys. Lett. **294**, 217 (1998).

[14] B. Cui, B. Lin, and S. A. Rice, J. Chem. Phys. **119**, 2386 (2003).

[15] G. M. Kepler and S. Fraden, Phys. Rev. Lett. **73**, 356 (1994).

[16] M. D. Carbajal-Tinoco, F. Castro-Roman, and J. L. Arauz-Lara, Phys. Rev. E **53**, 3745 (1996).

[17] J. C. Crocker and D. G. Grier, J. Colloid Interface Sci. **179**, 298 (1996).

[18] J. C. Crocker and D. G. Grier, Phys. Rev. Lett. **77**, 1897 (1996).

[19] R. Verma, J. C. Crocker, T. C. Lubensky, and A. G. Yodh, Phys. Rev. Lett. **81**, 4004 (1998).

[20] J. C. Crocker, J. A. Matteo, A. D. Dinsmore, and A. G. Yodh, Phys. Rev. Lett. **82**, 4352 (1999).

[21] P. Karnchanaphanurach, B. H. Lin, and S. A. Rice, Phys. Rev. E **61**, 4036 (2000).

[22] B. H. Lin, J. Yu, and S. A. Rice, Phys. Rev. E **62**, 3909 (2000).

[23] R. Verma, J. C. Crocker, T. C. Lubensky, and A. G. Yodh, Macromolecules **33**, 177 (2000).

[24] B. X. Cui, B. H. Lin, S. Sharma, and S. A. Rice, J. Chem. Phys. **116**, 3119 (2002).

[25] L. Starrs and P. Bartlett, Faraday Discuss. **123**, 323 (2003).

[26] H. N. W. Lekkerkerker and B. Widom, Physica A **285**, 483 (2000).

[27] T. T. M. Vo, L.-J. Chen, and M. Robert, J. Chem. Phys. **119**, 5607 (2003).

[28] C.-Y. Chou, B. C. Eng, and M. Robert, J. Chem. Phys. **124**, 044902 (2006).

[29] A. Ulman, *An Introduction to Ultrathin Organic Films from Langmuir-Blodgett to Self-Assembly* (Academic Press, Rochester, 1991).

[30] L. Wen and K. D. Papadopoulos, Colloids Surf., A **174**, 159 (2000).

[31] P. Hertz, Math. Ann. **67**, 387 (1909).

[32] H. Reiss, H. L. Frisch, and J. L. Lebowitz, J. Chem. Phys. **31**, 369 (1959).

[33] H. Reiss and R. V. Casberg, J. Chem. Phys. **61**, 1107 (1974).

[34] S. Torquato, B. Lu, and J. Rubinstein, J. Phys. A **23**, L103 (1990).

[35] S. Torquato and S. B. Lee, Physica A **167**, 361 (1990).

[36] S. Torquato, B. Lu, and J. Rubinstein, Phys. Rev. A **41**, 2059 (1990).

[37] S. Torquato, Phys. Rev. Lett. **74**, 2156 (1995).

[38] S. Torquato, Phys. Rev. E **51**, 3170 (1995).

[39] C.-Y. Chou, T.-C. Lee, S. Abel, D. R. Pilaski, and M. Robert (unpublished).

[40] S. Asakura and F. Oosawa, J. Chem. Phys. **22**, 1255 (1954).

[41] Y. L. Han and D. G. Grier, Phys. Rev. Lett. **91**, 038302 (2003).

[42] W. B. Russel, D. A. Saville, and W. R. Showalter, *Colloidal Dispersions* (Cambridge University Press, New York, 1989).

[43] T. Sugimoto, T. Takahashi, H. Itoh, S. Sato, and A. Muramatsu, Langmuir **13**, 5528 (1997).

[44] A. K. Arora and R. Rajagopalan, *Ordering and Phase Transitions in Charged Colloids* (VCH Publishers, New York, 1996).

[45] P. C. Hiemenz and R. Rajagopalan, *Principles of Colloid and Surface Chemistry* (Marcel Dekker, New York, 1997).

[46] C.-Y. Chou, Ph.D. thesis, Rice University, 2004.